Order online now!

www.rockland.com
tech@rockland.com
+1 484.791.3823

Datasheet for 100-4198

Biotin Antibody

Overview

Description:	Anti-Biotin (RABBIT) Antibody - 100-4198
Item No.:	100-4198
Size:	2 mL
Applications:	ELISA, EM, IF, Multiplex, Other, WB
Reactivity:	Biotin
Host Species:	Rabbit

Product Details

Background:	Biotin Antibody detects Biotin. Biotin is a water-soluble B-complex vitamin (vitamin B7). It is composed of a ureido (tetrahydroimidizalone) ring fused with a tetrahydrothiophene ring. A valeric acid substituent is attached to one of the carbon atoms of the tetrahydrothiophene ring. Biotin is a coenzyme for carboxylase enzymes, involved in the synthesis of fatty acids, isoleucine, and valine, and in gluconeogenesis. Biotin is necessary for cell growth, the production of fatty acids, and the metabolism of fats and amino acids. Anti-Biotin Antibody is ideal for investigators involved in Cell Signaling and Cell Biology research.
Synonyms:	rabbit anti-biotin antibody, rabbit anti biotin
Host Species:	Rabbit
Clonality:	Polyclonal
Format:	Antiserum

Target Details

Reactivity:	Biotin
Immunogen Type:	Native Protein
Immunogen:	Biotin conjugated to Keyhole Limpet Hemocyanin (KLH)
Purity/Specificity:	This product was prepared from monospecific antiserum by a delipidation and defibrination. Assay by immunoelectrophoresis resulted in a single precipitin arc against anti-rabbit serum, biotinylated IgG and Biotinylated BSA.

Application Details

Tested Applications:	ELISA
Suggested Applications:	EM, IF, Multiplex, Other, WB (Based on references)
Application Note:	Anti-Biotin has been tested in ELISA and is suitable for immunoblotting (western or dot blot), immunoprecipitation and most immunological methods requiring high titer and specificity.
Assay Dilutions:	All assays should be optimized by the user. Recommended dilutions (if any) may be listed below.
ELISA:	1:100,000
IHC:	User Optimized
WB:	1:10,000 - 1:25,000

Formulation

Physical State:	Lyophilized
Concentration:	90 mg/mL by Refractometry
Buffer:	0.01 M Sodium Phosphate, 0.15 M Sodium Chloride, pH 7.2
Preservative:	0.01% (w/v) Sodium Azide
Stabilizer:	None
Reconstitution Volume:	2.0 mL
Reconstitution Buffer:	Restore with deionized water (or equivalent)

Shipping & Handling

Shipping Condition:	Ambient
Storage Condition:	Store vial at 4° C prior to restoration. For extended storage aliquot contents and freeze at -20° C or below. Avoid cycles of freezing and thawing. Centrifuge product if not completely clear after standing at room temperature. This product is stable for several weeks at 4° C as an undiluted liquid. Dilute only prior to immediate use.
Expiration:	Expiration date is one (1) year from date of receipt.

Images

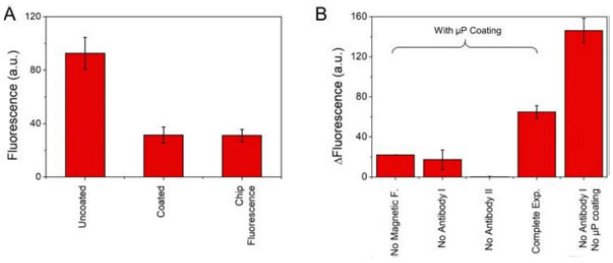

Figure
(a) Channels coating: remnant fluorescence due to nonspecific binding of anti-rabbit IgG labeled with B-rhodamine (p/n 611-1003) [AbII] at a concentration of 100 µg/ml in uncoated and coated microchannels with silane-PEG.
(b) Fluorescence obtained from the complete immunoassay at a flow rate of 5 µl/h and at a anti-biotin rabbit IgG (p/n 100-4198) [AbI] concentration of 50 pg/ml is compared to the fluorescence obtained from the immunoassay performed without applying the magnetic field (column 1), without adding anti-biotin rabbit IgG (p/n 100-4198) [AbI] (column 2), without adding), anti-rabbit IgG labeled with B-rhodamine (p/n 611-1003) [AbII] (column 3), and, finally, the efficacy of the microparticles coating was tested by performing the immunoassay without anti-biotin rabbit IgG (p/n 100-4198) [AbI] and with noncoated microparticles (column 5). The level of fluorescence of the two first columns in b results from nonspecific interactions of anti-rabbit IgG labeled with B-rhodamine (p/n 611-1003) [AbII] with the microparticles. Error bars are standard deviation. FIG. 5. PMID: 32038740.

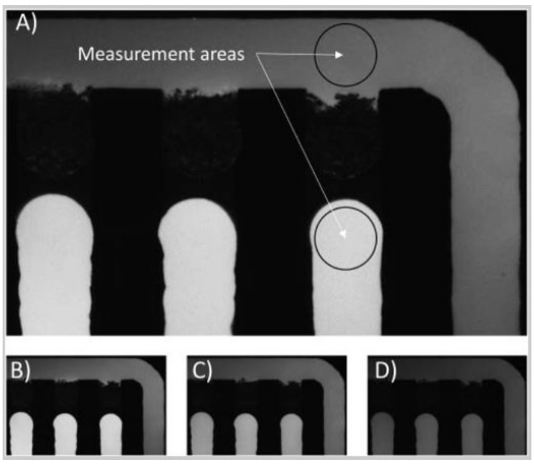

Figure
Typical experiment image where the complexes Ag–AbI–AbII are attached to the nanoparticles trapped in the magnetic traps and the fluorogenic substrate is flowed at different rates, where the measurement areas selected for the fluorescence analysis are shown. Measurement with a flow rate of (a) 1 µl/h, (b) 2 µl/h, (c) 5 µl/h, and (d) 10 µl/h. Experiment with anti-rabbit IgG labeled alkaline phosphatase was used (p/n 611-1502) and an anti-biotin rabbit IgG (p/n 100-4198) [AbI] concentration of 100 pg/ml. FIG. 6. PMID: 32038740.

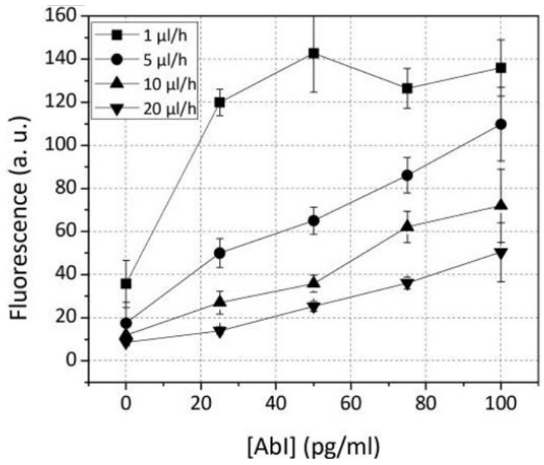

Figure
Shows the fluorescence difference from immunoassays at various concentrations of the primary antibody.
Calibration curve: fluorescence difference from immunoassays with varying concentrations of anti-biotin rabbit IgG (p/n 100-4198) [AbI] at different flow rates of the fluorogenic enzyme substrate anti-rabbit IgG labeled alkaline phosphatase was used (p/n 611-1502). Each experiment was repeated on three different devices. FIG. 7. PMID: 32038740.

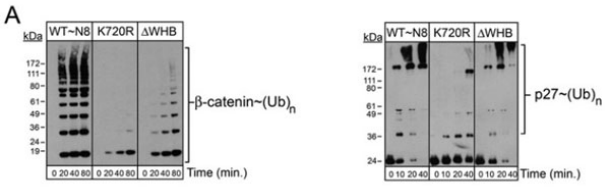

Western Blot
Western Blot of Anti-Biotin Antibody.
Functional analysis of mutations influencing RING conformational flexibility.
(A) Time-courses of polyubiquitination by SCFs reconstituted with fully-NEDD8ylated wild-type Cul1-Rbx1 (WT~N8), the non-NEDD8ylatable control (K720R), and the Cul1-Rbx1 WHB deletion mutant (ΔWHB). Left - SCFβTRCP-mediated polyubiquitination of a biotin-labeled β-catenin phosphopeptide, detected by western blotting with anti-biotin antisera. Right - SCFSkp2/CksHs1-mediated polyubiquitination of phospho-p27, detected by western blotting with anti-p27 antisera. Figure 5. PMID: 18805092.

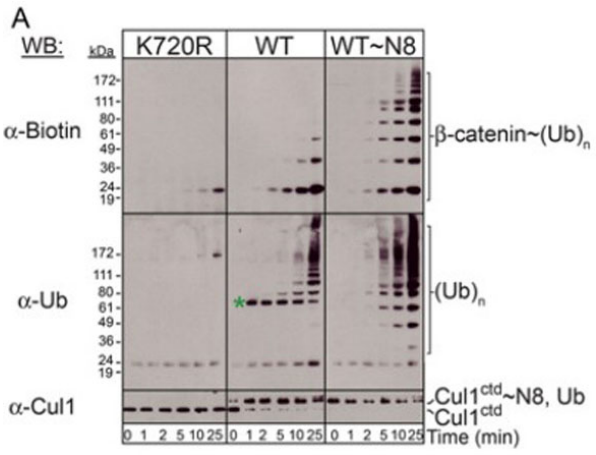

Western Blot
Western Blot of Anti-Biotin antibody.
Conformational control of CRL activities.
(A) Polyubiquitination reactions with SCFβTRCP/β-catenin phosphopeptide (left), and SCFSkp2/CksHs1/ phospho-p27 (right) reconstituted with non-NEDD8ylatable (K720R), un-NEDD8ylated wild-type (WT), and fully NEDD8ylated Cul1-Rbx1 (WT~N8). Reaction products were detected by immunoblotting, top panels with anti-biotin (left) or anti-p27 (right), middle with anti-His (Ubiquitin; green * - Cul1~Ubiquitin), and lower with anti-Cul1 C-terminus antisera. Figure 7. PMID: 18805092.

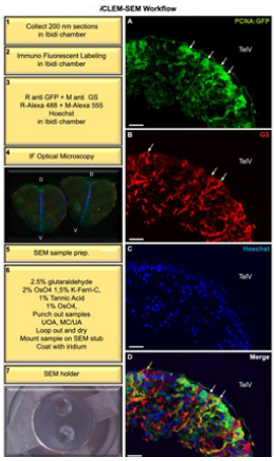

Immunofluorescence Microscopy
iCLEM-SEM workflow and immunofluorescent labelling on Tokuyasu chemical-fixed cryosections. Left: Major steps required for iCLEM-SEM workflow (steps 1–6). (A) Green Fluorescent Protein (GFP)-positive labelling (green) of proliferating cells from the Tg(PCNA:GFP) transgenic line (white arrows). (B) Glutamine Synthetase (GS)-positive labelling (red) of glial cells (white arrows). (C) Hoechst counterstaining (blue). (D) Multi-channel merge showing co-labelling of PCNA:GFP-positive cells with the glial marker (orange cells; white arrows) in the cytoplasm of a small number of cells. Differences in the intensity of antibody staining can additionally be noted (compare white arrows and yellow arrow). D dorsal; V ventral. TelV telencephalic ventricle. Scale bar (A–D) 20 µm. Fig 2. PMID: 33441723

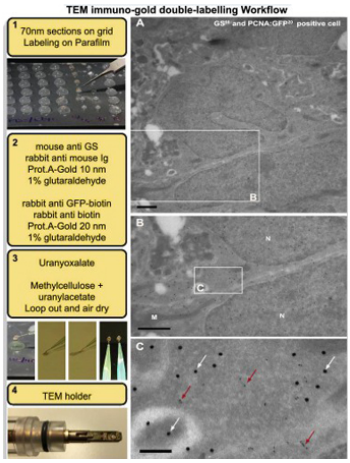

Immunofluorescence Microscopy
TEM immuno-gold double-labelling workflow and example of positive labelling on Tokuyasu chemical-fixed cryosections. Left: Major steps (1–4) required for TEM immuno-gold double-labelling workflow and associated images. (A,B,C) Cytosolic PCNA:GFP+/GS+ immuno-gold double-labelling at low (A) and high (B,C) magnifications demonstrating co-localization of the 10 nm (GS; red arrowheads) and 20 nm (PCNA:GFP; white arrowheads) particles. N, nucleus. Scale bar (A) 2 µm; (B,C) 200 nm. Fig 6. PMID: 33441723

References

- Lennartz HM et al. Visualizing suborganellar lipid distribution using correlative light and electron microscopy. *Nat Cell Biol.* (2026)
- Mukherjee R et al. Phosphoribosyl ubiquitination of SNARE proteins regulates autophagy during Legionella infection. *EMBO J.* (2025)
- Monster JL et al. β-catenin condensation facilitates clustering of the cadherin/catenin complex and formation of nascent cell-cell junctions. *Nat Commun.* (2025)
- Gómez-Sánchez R et al. Establishment of the phagophore–ERES membrane contact site initiates phagophore elongation. *Nat Struct Mol Biol.* (2025)
- Cong Y et al. Influenza A virus subverts the LC3-pericentrin dynein adaptor complex for host cytoplasm entry. *Sci Adv.* (2025)

- Filali-Mouncef Y et al. An APEX2-based proximity-dependent biotinylation assay with temporal specificity to study protein interactions during autophagy in the yeast Saccharomyces cerevisiae. *Autophagy.* (2024)
- Rudnik S et al. The lysosomal lipid transporter LIMP-2 is part of lysosome-ER STARD3-VAPB-dependent contact sites. *J Cell Sci.* (2024)
- Stajano D et al. Tetraspanin 15 depletion impairs extracellular vesicle docking at target neurons. *J Extracell Biol.* (2023)
- Ye S et al. Nogo receptor-Fc delivered by haematopoietic cells enhances neurorepair in a multiple sclerosis model. *Brain Commun.* (2023)
- Katheder NS et al. Nicotinic acetylcholine receptor signaling maintains epithelial barrier integrity. *Elife.* (2023)
- De Mazière A et al. An optimized protocol for immuno-electron microscopy of endogenous LC3. *Autophagy.* (2022)
- Tran NH et al. The stress-sensing domain of activated IRE1α forms helical filaments in narrow ER membrane tubes. *Science.* (2021)
- Li H et al. Cellular requirements for PIN polar cargo clustering in Arabidopsis thaliana. *New Phytol.* (2021)
- Oorschot V et al. TEM, SEM, and STEM-based immuno-CLEM workflows offer complementary advantages. *Sci Rep.* (2021)
- Zulkefli K et al. A role for Rab30 in retrograde trafficking and maintenance of endosome-TGN organization. *Exp Cell Res.* (2021)
- Cabukusta B et al. Human VAPome Analysis Reveals MOSPD1 and MOSPD3 as Membrane Contact Site Proteins Interacting with FFAT-Related FFNT Motifs. *Cell Rep.* (2020)
- Jongsma ML et al. SKIP-HOPS recruits TBC1D15 for a Rab7-to-Arl8b identity switch to control late endosome transport. *EMBO J.* (2020)
- Guevara-Pantoja PE et al. Micro–nanoparticles magnetic trap: Toward high sensitivity and rapid microfluidic continuous flow enzyme immunoassay. *Biomicrofluidics.* (2020)
- Landi A et al. Pseudomonas aeruginosa lectin LecB impairs keratinocyte fitness by abrogating growth factor signalling. *Life Sci Alliance.* (2019)
- Andres-Alonso M, Ammar MR, Butnaru I, et al. SIPA1L2 controls trafficking and local signaling of TrkB-containing amphisomes at presynaptic terminals. *Nat Commun.* (2019)
- Lee JY et al. Limiting Neuronal Nogo Receptor 1 Signaling during Experimental Autoimmune Encephalomyelitis Preserves Axonal Transport and Abrogates Inflammatory Demyelination. *J Neurosci.* (2019)
- Koerver L et al. The ubiquitin-conjugating enzyme UBE 2 QL 1 coordinates lysophagy in response to endolysosomal damage. *EMBO Rep.* (2019)
- McArthur K et al. BAK/BAX macropores facilitate mitochondrial herniation and mtDNA efflux during apoptosis. *Science.* (2018)
- Bower NI et al. Mural lymphatic endothelial cells regulate meningeal angiogenesis in the zebrafish. *Nat Neurosci.* (2017)
- Sztal et al. Zebrafish models for nemaline myopathy reveal a spectrum of nemaline bodies contributing to reduced muscle function. *Acta Neuropathologica* (2015)

- Henau et al. A redox signalling globin is essential for reproduction in Caenorhabditis elegans. *Nature Communications* (2015)
- Oorschot VMJ et al. Immuno correlative light and electron microscopy on Tokuyasu cryosections. *Methods Cell Biol.* (2014)
- Wolf E et al. Antisense-targeted immuno-EM localization of the pre-mRNA path in the spliceosomal C complex. *RNA.* (2012)
- Jubelin G et al. Pathogenic bacteria target NEDD8-conjugated cullins to hijack host-cell signaling pathways. *PLoS Pathog.* (2010)
- Jung, H et al. Detecting protein-ligand binding on supported bilayers by local pH modulation. *Journal of the American Chemical Society* (2009)
- Duda DM et al. Structural insights into NEDD8 activation of cullin-RING ligases: conformational control of conjugation. *Cell.* (2008)
- Peden AA et al. Localization of the AP-3 adaptor complex defines a novel endosomal exit site for lysosomal membrane proteins. *J Cell Biol.* (2004)
- Heijnen HFG et al. Concentration of rafts in platelet filopodia correlates with recruitment of c-Src and CD63 to these domains. *J Thromb Haemost.* (2003)
- Ohta H et al. One-step direct assay for mature-type adrenomedullin with monoclonal antibodies. *Clin Chem.* (1999)

Disclaimer

This product is for research use only and is not intended for therapeutic or diagnostic applications. Please contact a technical service representative for more information. All products of animal origin manufactured by Rockland Immunochemicals are derived from starting materials of North American origin. Collection was performed in United States Department of Agriculture (USDA) inspected facilities and all materials have been inspected and certified to be free of disease and suitable for exportation. All properties listed are typical characteristics and are not specifications. All suggestions and data are offered in good faith but without guarantee as conditions and methods of use of our products are beyond our control. All claims must be made within 30 days following the date of delivery. The prospective user must determine the suitability of our materials before adopting them on a commercial scale. Suggested uses of our products are not recommendations to use our products in violation of any patent or as a license under any patent of Rockland Immunochemicals, Inc. If you require a commercial license to use this material and do not have one, then return this material, unopened to: Rockland Inc., P.O. BOX 5199, Limerick, Pennsylvania, USA.